Astronomy & Astrophysics manuscript no. orionIII˙nsd2
January 19, 2013

© ESO 2013

arXiv:1104.3154v1 [astro-ph.SR] 15 Apr 2011

The chemical composition of the Orion star-forming region[⋆]

III. C, N, Ne, Mg and Fe abundances in B-type stars revisited

María-Fernanda Nieva[1⋆⋆] and Sergio Simón-Díaz[2,3]

[1] Max-Planck-Institut für Astrophysik, Karl-Schwarzschild-Str. 1, D-85741 Garching, Germany
[2] Instituto de Astrofísica de Canarias, E-38200 La Laguna, Tenerife, Spain
[3] Departamento de Astrofísica, Universidad de La Laguna, E-38205 La Laguna, Tenerife, Spain

ABSTRACT

Context. Early B-type stars are invaluable indicators for elemental abundances of their birth environments. In contrast to the surrounding neutral interstellar matter (ISM) and H ɪɪ regions their chemical composition is unaffected by depletion onto dust grains and by the derivation of different abundances from recombination and collisional lines. In combination with ISM or nebular gas-phase abundances they facilitate the otherwise inaccessible dust-phase composition to be constrained.
Aims. Precise abundances of C, N, Mg, Ne, Fe in early B-type stars in the Orion star-forming region are determined in order to: a) review previous determinations using a self-consistent quantitative spectral analysis based on modern stellar atmospheres and recently updated model atoms, b) complement results found in Paper I for oxygen and silicon, c) establish an accurate and reliable set of stellar metal abundances to constrain the dust-phase composition of the Orion H ɪɪ region in Paper II of the series.
Methods. A detailed, self-consistent spectroscopic study of a sample of 13 narrow-lined B0 V-B2 V stars in Ori OB1 is performed. High-quality spectra obtained with FIES@NOT are analysed using both a hybrid non-LTE method (classical line-blanketed LTE model atmospheres and non-LTE line formation) and line-profile fitting techniques, validating the approach by comparison with results obtained in Paper I using line-blanketed non-LTE model atmospheres and a curve-of-growth analysis.
Results. The comparison of the two independent analysis strategies gives consistent results for basic stellar parameters and abundances of oxygen and silicon. The extended analysis to C, N, Mg, Ne, and Fe finds a high degree of chemical homogeneity, with the 1σ-scatter typically adopting values of 0.03–0.07 dex around the mean for the various elements. Present-day abundances from B-type stars in Ori OB1 are compatible at similar precision with cosmic abundance standard values as recently established from early-type stars in the solar neighbourhood and also with the Sun.

Key words. Stars: abundances — Stars: atmospheres — Stars: early-type — Stars: fundamental parameters — Open clusters — Associations

1. Introduction

The Orion complex, containing the Orion molecular cloud and the Orion OB1 (Ori OB1) association, is one of the nearest Galactic regions with ongoing star formation, located at a distance of about 400 pc. It is unique for studying young massive stars, interstellar matter, and their interaction via feedback processes. The Orion complex can be regarded as the best reference for any further study of other star-forming regions. Its proximity and brightness have facilitated many detailed investigations, that yielded important discoveries and a wealth of information on many astrophysical phenomena over the past decades.

Blaauw (1964) divided Ori OB1 into four subgroups of stars, namely Ia, Ib, Ic and Id, distinguished by their different location in the sky and by their ages. Brown et al. (1994) derived mean ages of 11.4±1.9, 1.7±1.11, 4.6±2, and <1 Myr for subgroups Ia to Id, respectively. The youngest subgroup Ori OB1 Id is associated with the Orion nebula (M 42), the most studied H ɪɪ region and the closest ionized nebula to the Sun. The correlation between the ages of the stellar subgroups, their location, and the large scale structures in the interstellar medium around Orion OB1 have been interpreted as features of sequential star formation and the impact of type-II supernovae (Reynolds & Ogden 1979; Cowie et al. 1979; Brown et al. 1994).

Early B-type stars in Ori OB1 are important astrophysical objects that can be used to obtain present-day chemical abundances in terms of galactic chemical evolution. Moreover, the possibility of comparing the derived stellar abundances with those resulting from the spectroscopic analysis of the Orion nebula makes the tandem *massive stars in Ori OB1* and *M 42* a keystone in the investigation of the reliability of B-type stars and H ɪɪ regions as tracers of present-day abundances in the Universe.

First abundance determinations in B-type stars in Ori OB1 in the 90’s (Gies & Lambert 1992; Cunha & Lambert 1992, 1994; Kilian 1992; Gummersbach et al. 1998) indicated a large scatter up to 0.4 – 0.5 dex for O and Si, but also ≥ 0.2 dex for other elements such as C, N, and Fe. At that time, the most extensive work was carried out by Cunha & Lambert (1992, 1994), hereafter CL92 and CL94, respectively. They derived C, N, O, Si, and Fe abundances of 18 B-type main sequence stars from the four subgroups comprising the Ori OB1 association. They obtained a similar scatter in O and Si abundances as in the other cited works (based on smaller samples of stars), but also found

---

[⋆] Based on observations made with the Nordic Optical Telescope, operated on the island of La Palma jointly by Denmark, Finland, Iceland, Norway, and Sweden, in the Spanish Observatorio del Roque de los Muchachos of the Instituto de Astrofísica de Canarias.

[⋆⋆] Visiting researcher at Dr. Karl Remeis-Sternwarte & ECAP, Universität Erlangen-Nürnberg.

that the highest abundances were associated to some of the stars in the youngest (Id and some Ic) subgroups[1]. This abundance pattern was interpreted as an observational evidence supporting a scenario of induced star formation in which the new generation of stars are formed from interstellar material contaminated by type-II supernovae (SN II) ejecta.

This picture has changed substantially after new studies of oxygen and silicon abundances of early B-type stars in Ori OB1 by Simón-Díaz et al. (2006) and Simón-Díaz (2010, hereafter Paper I). Both stellar parameters and chemical abundances were shown to have different values than found previously, for the same stars. As a consequence, high chemical homogeneity of O and Si as derived from early B-type stars the Orion star-forming region is implied, and no clear indication for contamination with SN II nucleosynthesis products is found.

The results from Paper I for the mean abundance and standard deviation for O and Si are in full agreement with recent findings of homogeneous present-day chemical abundances in the solar neighbourhood (Przybilla, Nieva & Butler 2008, hereafter PNB08). There, a small but representative sample of early B-type stars was analysed, obtaining a significantly smaller scatter for C, N, O, Si, Mg, and Fe abundances than commonly found by previous studies.

Some reasons causing improvements in chemical abundance determinations of B-type stars can be found in Nieva & Przybilla (2010a,b), and references therein. In brief, these are a consequence of the minimization of systematic uncertainties of observational origin and from the spectral modeling and spectral analysis, with two main contributions: (a) the application of a *self-consistent* quantitative spectral analysis, i.e. to derive stellar parameters and chemical abundances from the spectrum only, without resorting to any extra ingredient like a photometric effective temperature estimation, and (b) the reliability of the atomic models and the selection of appropriate diagnostic lines for the stellar parameter and abundance determination.

In view of the results obtained in Paper I and PNB08 a revision of abundances of other important elements in Ori OB1 stars is warranted. The main aim of this third paper of the series, in combination with Paper I, is to establish an accurate and reliable set of abundances for C, N, O, Ne, Mg, Si, and Fe in early B-type stars in the Orion star-forming region, providing a basis to perform a thorough comparison between stellar and nebular chemical abundances in the Orion star-forming region Simón-Díaz & Stasińska (2011, hereafter Paper II of this series).

The analysis presented in this paper is based on recently updated model atoms for non-LTE calculations (see Table 1) which have been already applied in a small sample of early B-type stars in the solar neighbourhood (PNB08) and more recently in a larger sample (Nieva & Przybilla, in prep.). These model atoms are not available at present in the stellar atmosphere code used in Paper I, therefore, we decided to base the analysis on the codes and techniques described in PNB08. For consistency, we performed the whole analysis from scratch (also including the stellar parameters, and O and Si abundance determination). The comparison of results referent to stellar parameters, O and Si abundances obtained by two independent analyses will be very valuable to reinforce the conclusions presented in Paper I and/or investigate possible biases originated by the use of different stellar atmosphere codes and methodologies.

The paper is structured as follows: Sect. 2 briefly describes the star sample and the observations. The spectrum synthesis in non-LTE and the codes used in the present work are described in Sect. 3. The self-consistent quantitative spectral analysis is summarized in Sect. 4. Sect. 5 resumes the results and the comparison with other representative works in the literature. A summary is given and the conclusions are discussed in Sect. 6. An example of a global spectrum synthesis for one star of the sample is given in Appendix A.

2. The star sample

The star sample consists of 13 early B-type main sequence stars of spectral classes B0 V to B2 V and low projected rotational velocities ($v \sin i \leq 60$ km s^{-1}) in the Ori OB1 association. The spectroscopic dataset used in this study is the same presented in Paper I. It refers to high resolution and high signal-to-noise ratio spectra obtained with the Fibre-fed Echelle Spectrograph (FIES) attached at the 2.5m Nordic Optical Telescope (NOT) in El Roque de los Muchachos observatory on La Palma (Canary Islands, Spain) in November, 2008. Details of the data reduction process and the quality of the spectra can be found in Paper I.

3. Spectrum synthesis in non-LTE

The non-LTE line-formation computations follow the methodology discussed in detail in our previous studies for H, He and C (Nieva & Przybilla 2007, 2008) and for N, O, Ne, Mg, Si and Fe (PNB08). In brief, a hybrid non-LTE approach is employed, i.e. combining classical line-blanketed LTE model atmospheres and non-LTE line-formation calculations. This technique provides an efficient way to compute realistic synthetic spectra in all cases where the atmospheric structure is close to LTE, as it is the case for the early B-type main sequence stars analysed here (Nieva & Przybilla 2007).

The model atmospheres were computed with the Atlas9 code (Kurucz 1993b) which assumes plane-parallel geometry, hydrostatic, radiative and local thermodynamic equilibrium, and chemical homogeneity. Solar abundances of Grevesse & Sauval (1998) were adopted in the atmospheric structure[2] computations. Line blanketing was realized here by means of opacity distribution functions ODFs (Kurucz 1993a) with solar abundances scaled to Grevesse & Sauval (1998). The model atmospheres were held fixed in the subsequent non-LTE calculations.

Non-LTE level populations and model spectra were obtained with recent versions of Detail and Surface (Giddings 1981; Butler & Giddings 1985); both updated by K. Butler. The coupled radiative transfer and statistical equilibrium equations were solved with Detail, employing an accelerated lambda iteration scheme of Rybicki & Hummer (1991). This allows even complex ions to be treated in a realistic and efficient way. Synthetic spectra were then calculated with Surface, using refined line-broadening theories. The sources of model atoms adopted for the present work are listed in Table 1. Details on the updates are given in by Nieva & Przybilla (in prep.).

Continuous opacities due to hydrogen and helium were considered in non-LTE and metal line blocking was accounted for in LTE via Kurucz' ODFs. Microturbulence was considered in a consistent way throughout all computation steps: selection of

---

[1] For other elements the scatter was also relatively large (e.g. 0.2, 0.45, and 0.35 dex for C, N, and Fe, respectively), but they did not find significant variations of abundances across the subgroups.

[2] The effect of the 'new' solar abundances (Asplund et al. 2009) on the atmospheric structure and on the ODF's is weak.

Table 1. Model atoms for non-LTE calculations.

Ion	Model atom
H	Przybilla & Butler (2004)
He I/II	Przybilla (2005)
C II-IV	Nieva & Przybilla (2006, 2008)
N II	Przybilla & Butler (2001)*
O I/II	Przybilla et al. (2000), Becker & Butler (1988a)*
Ne I/II	Morel & Butler (2008)*
Mg II	Przybilla et al. (2001)
Si III/IV	Becker & Butler (1990a)
Fe II/III	Becker (1998), Morel et al. (2007)*

* Updated by N. Przybilla (priv. comm.)

Table 2. Spectroscopic indicators for the $T_{\rm eff}$ and $\log g$ determination. The boxes indicate ionization equilibria that have been quantitatively matched in the analysis.

#	Object	H	He I	He II	C II	C III	C IV	O I	O II	Ne I	Ne II	Si III	Si IV	Fe II	Fe III
1	HD36512	●	●	●	●	●	●		●		●	●	●		●
2	HD37020	●	●	●	●	●			●	●	●	●	●		●
3	HD36960	●	●	●	●	●			●	●	●	●	●		●
4	HD37042	●	●	●	●	●			●	●	●	●	●		●
5	HD36591	●	●	●	●	●		●	●	●	●	●	●		●
6	HD36959	●	●	●	●	●		●	●	●	●	●	●		●
7	HD37744	●	●		●	●		●	●	●	●	●	●	●	●
8	HD35299	●	●		●	●		●	●	●		●	●	●	●
9	HD36285	●	●		●	●		●	●	●		●	●	●	●
10	HD35039	●	●		●	●		●	●	●		●	●	●	●
11	HD36629	●	●		●	●		●	●	●		●		●	●
12	HD36430	●	●		●	●		●	●	●		●		●	●
13	HD35912	●	●		●	●		●	●	●		●		●	●

appropriate ODFs for line blanketing and line blocking, atmospheric structure calculations, determination of non-LTE populations and formal solution.

Grids of synthetic spectra for H/He, C, N, O, Mg and Si have been computed in order to speed up the analysis. They cover effective temperatures from 15 000 to 35 000 K in steps of 1000 K, surface gravities from 3.0 to 4.5 in steps of 0.1 dex, microturbulences from 0 to 8 km s^{-1} in steps of 2 km s^{-1} (for H/He, Si and O microturbulence reaches a value of 12 km s^{-1}) and metal abundances within 1 dex centered on the Cosmic Abundance Standard proposed in PNB08 in steps of 0.1 dex. Hydrogen and helium abundances adopt PNB08 values. The lower limit of the surface gravity for each value of temperature/microturbulence was constrained by the convergence of Atlas9. All grids have been successfully tested by reproducing results from PNB08 within a broad temperature range. Micro-grids varying abundances only, were computed per star for neon and iron once all stellar parameters have been determined with the larger precomputed grids.

4. Self-consistent quantitative spectral analysis

The analysis method used in this paper is based on a spectral line-fitting procedure[3]. We aim at deriving atmospheric parameters and chemical abundances self-consistently by reproducing several independent spectroscopic indicators simultaneously. The atmospheric parameters primarily derived here are the effective temperature $T_{\rm eff}$, surface gravity $\log g$, microturbulence ξ, macroturbulence ζ, projected rotational velocity $v \sin i$, elemental abundances ε(X).

The quantitative analysis is mostly automatized, but it also allows to work interactively in some decisive steps. The interpolation in stellar parameters via spectral line fitting using χ^2-minimization within the precomputed grids is performed with the program Spas[4]. The code allows flexible selection of spectroscopic indicators for parameter determinations which may vary from star to star upon availability of specific spectral lines. Linelists can also be chosen interactively. This is crucial since then problematic spectral lines, i.e. too weak, blended, with low S/N, in a region where the continuum normalization is difficult or with a particular shortcoming in the spectral synthesis can be excluded. The local continuum can also be adjusted interactively. This might slow down the analysis process in cases where the linelist is long but the gain in precision is high.

The strategy used for the analysis of our star sample is as follows. A first estimation of $T_{\rm eff}$ and $\log g$ is obtained by means of a simultaneous fit to most H and He lines (an accuracy better than ~ 5% and 0.1–0.2 dex, respectively, is expected for the case of this high quality set stellar spectra). Then the procedure starts to consider lines of other elements to end up with a self-consistent solution for atmospheric parameters and chemical abundances, also including an estimation of their internal errors. In this second step, every element is analysed independently and some interactive iterations to fine-tune the stellar parameter determination are needed in order to find a unique solution for all indicators.

Numerous metal lines were analysed simultaneously per star/element. The high S/N and high resolution spectra, the optimum continuum normalization, the ample wavelength range coverage, the presence of many unblended sharp spectral lines and the adoption of our updated model atoms for spectral synthesis calculations allow us to analyse more lines than in standard works. The linelist varies slightly from star to star because the selection of good lines to be analysed depends on the temperature, the quality of the spectra and the wavelength coverage. In particular, the line lists used to derive final values of elemental abundances has been chosen for each star, in a way that the abundance from any line does not differ by more than ~2–3σ from average.

Ionization equilibria, i.e. the requirement that lines from different ions of an element have to indicate the same chemical abundance, along with the fitting of the wings of the H Balmer lines facilitate a fine-tuning of the previously derived parameters. Whenever possible, we use multiple ionization equilibria for the parameter determination as the redundancy of information helps to minimize systematic errors. In particular, we have found that the use of more than one ionization equilibrium helps to better constraint the surface gravity compared to the case when only H lines are used.

The selection of ionization equilibria to be analysed depends on the temperature range of the star. Table 2 summarizes the available indicators[5] for the star sample. Note that the use of more than one ionization equilibrium has been always possible. In addition, the availability of the Fe II/III ionization equilibrium allow to also impose a constraint to the metallicity, [M/H] $\simeq$ [Fe/H].

---

[3] Note that we used here a different approach than in Paper I. More details can be found in Sect. 5.1.

[4] Spectrum Plotting and Analysing Suite (Spas, Hirsch 2009).

[5] Note that we analyse Si III/IV lines only because the model atom employed here does not produce reliable Si II lines (see also Paper I).

Table 3. Stellar parameters and elemental abundances of the program stars.

			FW		ADS					log X/H + 12 (NLTE, ADS)					
Target	SpT	Sub-Gr.	$T_{\rm eff}$ (K)	$\log g$ (cgs)	$T_{\rm eff}$ (K)	$\log g$ (cgs)	ξ	vsini ($\mathrm{km\,s^{-1}}$)	ζ	C	N	Ne	Mg	Fe	#
36512	B0 V	Ic	33700	4.2	33400 ± 300	4.30 ± 0.07	4 ± 1	20 ± 1	10 ± 2	8.36 ± 0.15	7.83 ± 0.15	8.16 ± 0.10	7.51	7.55 ± 0.02	1
37020	B0.5 V	Id	30500	4.2	30700 ± 300	4.30 ± 0.08	0 ± 1	45 ± 3	20 ± 5	8.40 ± 0.07	7.85 ± 0.09	8.09 ± 0.08	7.64	7.53 ± 0.08	2
36960	B0.5 V	Ic	28900	3.9	29000 ± 350	4.10 ± 0.08	4 ± 1	28 ± 2	20 ± 6	8.39 ± 0.07	7.78 ± 0.08	8.13 ± 0.09	7.61	7.53 ± 0.11	3
37042	B0.7 V	Id	29700	4.2	29300 ± 300	4.30 ± 0.09	2 ± 1	30 ± 2	10 ± 3	8.33 ± 0.11	8.04 ± 0.08	8.13 ± 0.09	7.64	7.54 ± 0.09	4
36591	B1 V	Ib	27200	4.1	27000 ± 250	4.12 ± 0.05	2 ± 1	12 ± 1	...	8.30 ± 0.10	7.81 ± 0.09	8.10 ± 0.07	7.61 ± 0.02	7.49 ± 0.12	5
36959	B1 V	Ic	25900	4.2	26100 ± 200	4.25 ± 0.07	0 ± 1	12 ± 1	5 ± 1	8.37 ± 0.11	7.85 ± 0.09	8.18 ± 0.10	7.66 ± 0.04	7.53 ± 0.11	6
37744	B1.5 V	Ib	23800	4.1	24000 ± 400	4.10 ± 0.10	0 ± 1	33 ± 2	15 ± 2	8.32 ± 0.07	7.81 ± 0.10	8.12 ± 0.08	7.58	7.52 ± 0.07	7
35299	B1.5 V	Ia	23700	4.2	24000 ± 200	4.20 ± 0.08	0 ± 1	8 ± 1	...	8.37 ± 0.07	7.81 ± 0.07	8.12 ± 0.09	7.61 ± 0.07	7.49 ± 0.10	8
36285	B2 V	Ic	20600	4.0	21700 ± 300	4.25 ± 0.08	0 ± 1	11 ± 1	8 ± 1	8.32 ± 0.07	7.77 ± 0.09	8.04 ± 0.08	7.52 ± 0.08	7.54 ± 0.10	9
35039	B2 V	Ia	19800	3.7	19600 ± 200	3.56 ± 0.07	4 ± 1	12 ± 1	7 ± 1	8.34 ± 0.10	7.77 ± 0.09	8.04 ± 0.08	7.49 ± 0.06	7.48 ± 0.10	10
36629	B2 V	Ic	20000	4.1	20300 ± 400	4.15 ± 0.10	2 ± 1	10 ± 1	5 ± 1	8.36 ± 0.07	7.82 ± 0.08	8.02 ± 0.09	7.50 ± 0.02	7.52 ± 0.11	11
36430	B2 V	Ic	18600	4.1	19300 ± 200	4.14 ± 0.05	0 ± 1	20 ± 2	10 ± 2	8.32 ± 0.08	7.76 ± 0.10	8.03 ± 0.12	7.54 ± 0.05	7.50 ± 0.07	12
35912	B2 V	Ia	18500	4.0	19000 ± 300	4.00 ± 0.10	2 ± 1	15 ± 1	8 ± 1	8.33 ± 0.09	7.76 ± 0.07	8.05 ± 0.11	7.50 ± 0.05	7.52 ± 0.08	13

Notes. Target id are HD numbers. Parameters derived with Fastwind (FW, Paper I) and Atlas+Detail+Surface (ADS, this work) are listed. Uncertainties in parameters from Paper I are similar than in the present work.

Table 4. Average metal abundances.

	This work	Paper I	PNB08	$\mathrm{CL94^{NLTE}}$	$\mathrm{CL94^{LTE}}$	Sun[a]
C	8.35±0.03 [0.09]		8.32±0.03	8.40±0.11	8.35±0.06	8.47±0.05
N	7.82±0.07 [0.09]		7.76±0.05	7.76±0.13	7.79±0.11	7.87±0.05
O	8.77±0.03 [0.10]	8.73±0.04	8.76±0.03	8.72±0.13	8.73±0.13	8.73±0.05
Ne	8.09±0.05 [0.09]		8.08±0.03	8.11±0.04[b]	...	7.97±0.10
Mg	7.57±0.06 [0.05]		7.56±0.05	...	...	7.64±0.04
Si	7.50±0.06 [0.06]	7.51±0.03	7.50±0.02	7.14±0.13	7.36±0.14	7.55±0.03
Fe	7.52±0.02 [0.09]		7.44±0.04	...	7.47±0.10	7.54±0.04

Notes. Average metal abundances, 1-σ uncertainties and intrinsic uncertainties for each element (in brackets) derived in this work are compared to values from Paper I, the present-day Cosmic Abundance Standard by PNB08, abundances in NLTE and LTE of 17 stars in Ori OB1 by CL94, and solar abundances. (a) Protosolar values by AGSS09 (Table 5 in the original paper). (b) Value from 16 stars, from CHL06.

The fine-tuning of microturbulence, stellar parameters and abundances is performed at the same time. In particular, microturbulence is determined by imposing a zero correlation between individual line abundances for some ions.

The strength of this analysis method is that most important sources of systematic uncertainties can be identified and the remaining errors reduced to minimum values. See Nieva & Przybilla (2010a,b) for more detailed discussions on the methodology and systematic errors in the spectral analysis of this kind of stars.

5. Our results for the Orion B-type stars and comparison with previous work

Table 3 summarizes atmospheric parameters and elemental abundances of C, N, Ne, Mg and Fe derived in this study for the 13 sample stars. There, also spectral type and subgroup to which the stars belong within Ori OB1 are given. The identification numbering of the stars (last column) follows the one used in Paper I. The corresponding mean values and 1-σ uncertainties derived from the whole star sample are presented in first column of Table 4. Note that mean abundances for O and Si obtained in this work are also indicated. These abundances (though not presented in Table 3) were derived for completeness, and to be compared with those obtained in Paper I (see Sect. 5.1).

Table 4 also contains information about results obtained by previous studies of early B-type stars in Ori OB1 from Paper I, CL92, CL94 and Cunha et al. (2006), hereafter CHL06, early B-type stars in the solar neighbourhood from PNB08, and the set of protosolar abundances proposed by Asplund et al. (2009), hereafter AGSS09. Values from CL94 in Table 4 have been computed from their total sample and are slightly different than those values indicated by them, calculated from a sub-sample of their work. A detailed discussion on the comparison of results from the analysis performed here and the various cited studies is presented in the following sub-sections.

¿From inspection of Tables 3 and 4 it can be concluded that the large scatter in abundances found for C, N, and Fe by previous works (see Sect. 1) has been significantly reduced. In addition, the high degree of homogeneity of derived abundances for all the analysed elements is remarkable (the 1-σ dispersion associated to the mean value of the whole sample is always significantly smaller than the intrinsic uncertainties from the individual analysis, obtained by averaging the individual errors for each star listed in Table 3. These values are indicated in brackets in Table 4). To better illustrate these conclusion, we plot in Fig. 2, the individual abundances for the analysed Ori OB1 stars (black filled squares) together with the 1-σ dispersion of abundances derived from the whole sample (grey-shaded area), and compare them with other studies listed in Table 4.

5.1. B stars in Ori OB1: Paper I

The same set of observed spectra was analysed in Paper I and in the present work. The method used here based on Atlas+Detail+Surface and the one adopted in Paper I

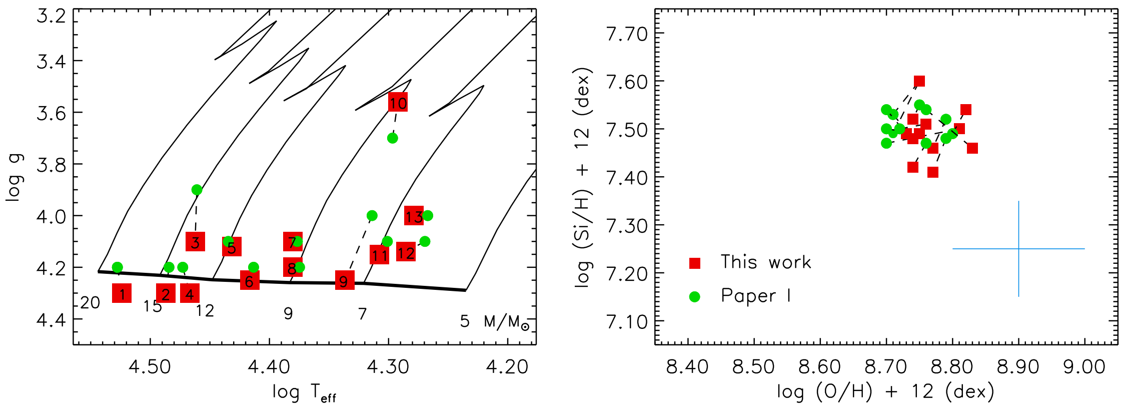

Fig. 1. Comparison of effective temperature and surface gravities (left panel) and oxygen and silicon abundances (right panel) derived in Paper I with Fastwind and the present work with Atlas+Detail+Surface. Evolutionary tracks (corresponding to Z=0.02) are extracted from Schaller et al. (1992). Numbers in the left panel identify the stars, as in Table 3 The blue cross in the right panel indicates the typical uncertainties in O and Si abundances from individual analyses.

(Fastwind) employ the same philosophy: the simultaneous determination of stellar parameters and chemical abundances from the spectrum only. However, the codes and the spectral analysis are different. Results of Paper I are based on the unified atmosphere code Fastwind (Puls et al. 2005) that models the stellar atmosphere and wind in non-LTE. The input atomic data for the line formation of hydrogen, helium, silicon and oxygen are not identical to the ones used here. Furthermore, the determination of chemical abundances in Paper I was based on equivalent widths and the curves of growth, while here direct spectral line fits are performed. Finally, the spectroscopic diagnostics used for the stellar parameters determination are different: on the one hand, Paper I relies exclusively on the H Balmer lines, along with the He i/ii and/or Si ii/iii/iv ionization equilibria; on the other hand, as described in Sect.4, the analysis presented in this paper uses all available ionization equilibria for He, Si, C, N, O, Ne, and Fe.

Stellar parameter and oxygen and silicon abundance determinations were carried out independently to the work in Paper I, without a priori information of final results. The comparison of both studies can be found in Tables 3 (stellar parameters) and 4 (mean abundances and 1-σ dispersion), and Figs. 1 and 2. In spite of all differences in the two analyses, the similarity of results derived in both works is remarkable. The global agreement in the four quantities, $T_{\rm eff}$, $\log g$, ϵ(O), and ϵ(Si), is very good within the uncertainties.

Fig. 2 shows a detailed comparison of abundances for the 13 sample stars with results for O and Si from Paper I (red open squares) for the same objects. The analysed stars are separated in the various Ori OB1 stellar subgroups. No trend in O or Si is found, confirming the conclusions of Paper I of chemical homogeneity of these elements in the region. We refer the reader to Paper I for a similar comparison with results from CL92 and CL94. The differences of mean abundances for the sample is 0.04 dex for oxygen and 0.01 dex for silicon, that within the errors are negligible, and the 1-σ dispersion of abundances in the whole sample obtained in both analysis is similar (see Table 4).

5.2. B stars in Ori OB1: Cunha et al.

The chemical composition of the Orion star forming region derived by CL94 has been a commonly used reference for several applications in contemporary astrophysics for the past two decades. They derived LTE and non-LTE abundances for a sample of 18 B-type stars. Both analyses were based on a photometric determination of the effective temperature. LTE abundances were obtained using ATLAS6 line blanketed model atmospheres (Kurucz 1979). Non-LTE abundances were derived using a similar strategy as in the present work, as described in Sect. 4; i.e Detail and Surface NLTE computations on top of a line blanketed LTE atmospheric structure. Details on the non-LTE computations used by CL94 can be found in the original papers by Becker & Butler (1988b, 1989, 1990a,b) and Eber & Butler (1988). Two main differences distinguish our NLTE computations from those used by CL94: on the one hand, older versions of the codes and mostly older atomic data (our model atoms are listed in Table 1), except for the Si model atom that is the same for both works; and on the other hand, their non-LTE line formation was computed on top of the slightly blanketed LTE Gold (1984) atmospheric structures, while we use the fully blanketed ATLAS9 model.

In CL94, the idea of self-enrichment via supernovae explosions was very attractive to explain discrepant abundances between star members of the region. This explanation to the chemical patterns found by CL92 and CL94 has been challenged by new results from Simón-Díaz et al. (2006) and Paper I. There, highly homogeneous O and Si abundance was found for Ori OB1, with no clear indications of SN-II contamination. The high degree of homogeneity is confirmed here by means of an independent spectroscopic analysis.

A comparison of C, N, and Fe abundances derived from our analysis, with those provided by CL94 (both NLTE[6] and LTE) is presented in Table 4 (mean abundances and 1-σ dispersions) and Fig. 2 (star-by-star abundances). Despite the differences in the methods, codes and observed spectra, the mean values of the present work and those from CL94 for C, N, O, and Fe, both in non-LTE and in LTE, are in agreement within the uncertainties. Our chemical abundances are, however, more precise thanks to the improvements in reducing several systematic effects in the whole procedure (Nieva & Przybilla 2010a,b). In particular, Fig. 2 shows significant differences in the derived abundances for individual stars, e.g. of up to 0.3 dex in some stars for the case of C and N from CL94, in contrast to our results. It is also remarkable the case of iron, where we find a certainly smaller scatter compared to their LTE determinations. Only one element

---

[6] The NLTE abundances have been the preferred cited values in the literature

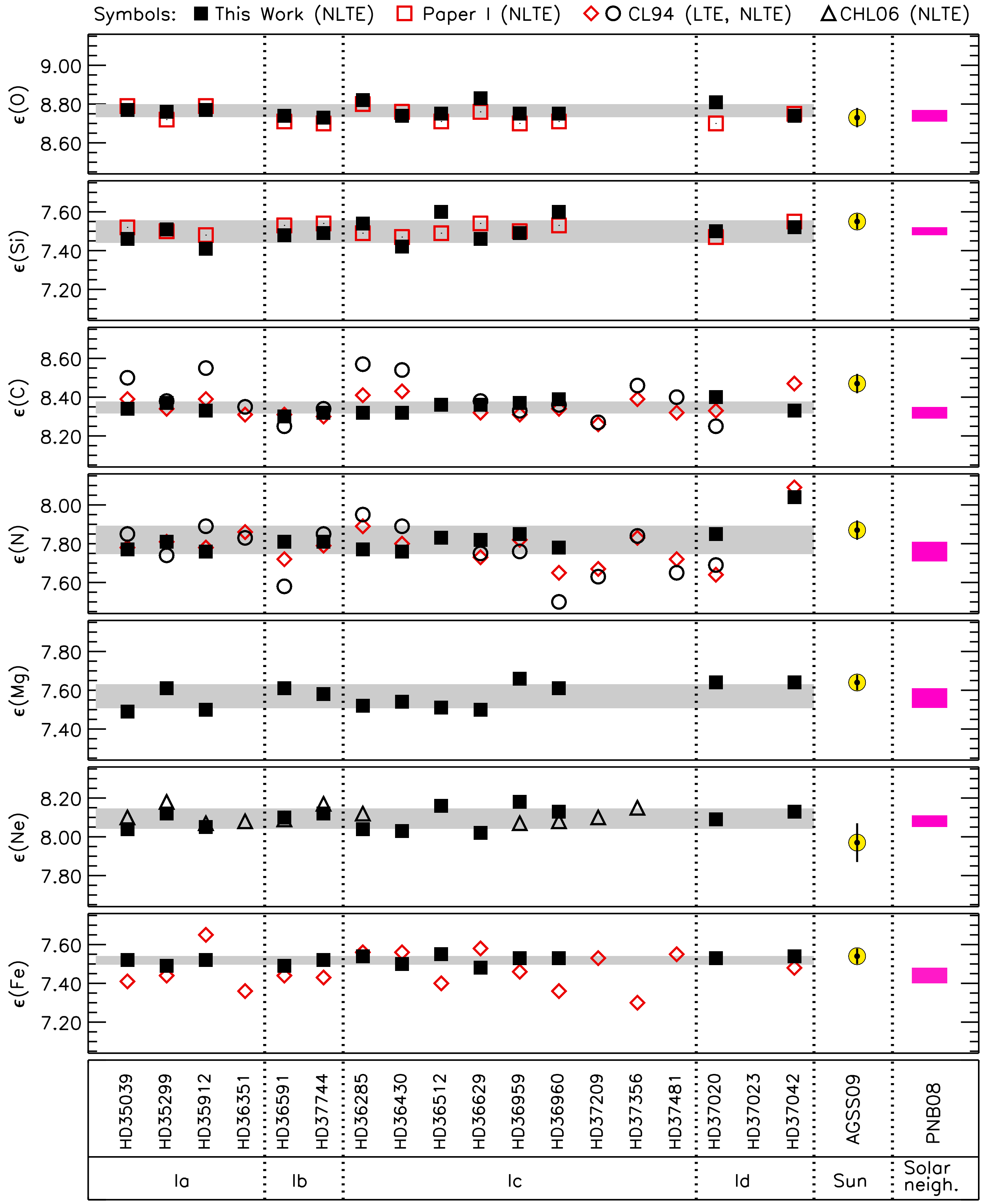

Fig. 2. Elemental abundances in our Ori OB1 sample stars and a comparison with previous work, and with common abundance standards. Symbols for data from this work, Paper I, CL94 and CHL06 are explained in the upper part of the figure. The grey-shaded region represents the 1-σ dispersion of abundances from the whole sample of 13 stars. Protosolar values of AGSS09 and the Cosmic Abundance Standard of PNB08 are given on the right hand side of the figure for comparison.

has drastically changed its mean abundance: silicon. The discrepancy of Si abundance is probably related to the combined effect of an inaccurate determination of the effective temperature and the use of certain diagnostic lines, traditionally used to establish the microturbulence and derive the Si abundance, which have been identified to be problematic (see Paper I for more details).

In a more recent work by CHL06, non-LTE Ne abundances for a sub-sample of stars in CL94 were derived using the previously determined stellar parameters and synthetic spectra computed with Tlusty (Hubeny 1988; Hubeny & Lanz 1995). In brief, the code calculates the stellar structure and the line formation simultaneously in NLTE. The non-LTE atmospheric structures from Tlusty are in agreement to better than 1% with those from ATLAS9, in LTE, for temperatures up to (at least) ~35,000 K (see Nieva & Przybilla 2007). Therefore the main difference to our work is the input atomic data for the line formation. Moreover, their abundances were derived from Ne i, while ours were determined from Ne i and Ne ii, that allowed us to analyse the hotter objects. A good agreement (star-by-star, and therefore mean abundances and scatter) is obtained between our Ne abundances and those derived in CHL06.

5.3. B-type stars in the Solar neighbourhood

The chemical abundances of the star sample agree very well with the recently proposed Present-Day Cosmic Abundance Standard of the solar neighbourhood, obtained from a representative group of early B-type stars in associations and the field by PNB08 (see Table 4 and Fig. 2). This agreement strengthens the idea that chemical homogeneity is naturally found in the solar neighbourhood once most prominent systematic uncertainties of stellar parameters and abundances have been minimized. These results are also confirmed by the study of a larger sample of B-type stars in the solar neighbourhood (Nieva & Przybilla, in prep.).

5.4. The Sun

Table 4 and Fig. 2 show the overall agreement between present-day metal abundances in the Orion star-forming region as derived here from early B-type stars and solar[7] values by Asplund et al. (2009), despite some small remaining discrepancies.

Comparisons of chemical composition of young early B-type stars and a much older star like our Sun have a historical character, since the Sun is the preferred reference for the chemical abundances in most astrophysical applications. There are, however, several issues related to the Sun in context of Galactochemical evolution that are still not well understood, e.g. whether the Sun has actually migrated from its nursery to the current location in the Galaxy (Portegies Zwart 2009; Schönrich & Binney 2009), or some small-scale peculiarities in the solar abundance pattern in comparison with solar analogs (Meléndez et al. 2009; Ramírez et al. 2009). The metal enrichment of the interstellar matter since the Sun's formation is also not precisely known, but a good estimate may be achieved via Galactic chemical evolution models. The agreement of chemical abundances derived from early B-type stars and the protosolar values indicate that there has been no significant local chemical enrichment since the formation of the Sun or that the Sun has been formed in another region – see also c.f. Carigi & Peimbert (2010).

We leave this discussion for the upcoming work on a larger sample of early B-type stars in the solar neighbourood distributed in various OB associations and the local field (Nieva & Przybilla, in prep.)

5.5. Late-type stars in Ori OB1

Late-type stars are other abundance indicators than the Sun to compare with our present-day abundances derived for the Orion star-forming region. The main differences of these stars with our Sun is that they have been indeed formed from the same material than the early B-type stars studied here and that they should be younger than the Sun because they belong to a young association. There are however a few issues to bear in mind when evaluating chemical abundances of cooler stars. Elemental abundances determined for late-type stars are usually not absolute values, like in this work, but they are derived relative to a reference, which in most cases is the Sun. At present, atmospheric codes accounting for 3D effects, relevant for stars with convective envelopes, or a non-LTE treatment of chemical elements are not implemented for most analyses of late-type stars other than the Sun. In spite of these issues, for completeness and to have a general picture of the Orion star-forming region, we cite a few recent works on the chemical composition of late-type stars in Ori OB1 and compare them with our results.

González Hernández et al. (2008), D'Orazi et al. (2009), and Biazzo et al. (2010) have recently obtained Fe abundances[8] in late-type stars in Ori OB1b and the Orion Nebula Cluster (ONC = Ori Ob1d). The three studies remark the small scatter in the derived abundances within each subgroup. For Ori OB1b, González Hernández et al. and Biazzo et al. derive 7.48 ± 0.09 and 7.46 ± 0.05 dex, respectively, while D'Orazi et al. find hints (only 1 star analysed) for subsolar metallicity. For stars in the ONC, D'Orazi et al. obtain 7.49 ± 0.07 dex, and Biazzo et al., 7.41 ± 0.11 dex. As argued by Biazzo et al., these discrepancies may be due to systematic effects in the analysis. For example, it is remarkable that the re-analysis by Biazzo et al. of some of the stars in the ONC analysed by D'Orazi et al. led to differences up to 0.13 dex in some cases. Our present-day abundance of iron is in agreement with results from the analysis of late-type stars in Ori OB1.

6. Summary and conclusions

We determined the stellar parameters and H, He, C, N, O, Ne, Mg, Si and Fe abundances of a sample of 13 early B-type stars in the Ori OB1 star-forming region by means of a detailed, self-consistent spectroscopic analysis. We applied an updated spectral synthesis in non-LTE based on a hybrid non-LTE approach using Atlas9 line blanketed LTE model atmospheres, non-LTE Detail+Surface line formation calculations, and line-fitting analysis techniques. We used lines from different ionization stages of these elements where possible, and treated carefully several sources of systematic errors – summarized in Nieva & Przybilla (2010a,b) – in order to obtain accurate and reliable results and minimize as much as possible the final uncertainties.

---

[7] Note that protosolar abundances have been chosen because they represent the chemical composition at the Sun-formation time.

[8] The original papers provide Fe abundances on a [Fe/H] scale. We used the solar Fe abundances indicated in each study to compute the Fe abundances in the same scale used in this work.

The stellar parameters derived here agree with those determined in Paper I of this series using the non-LTE, line-blanketed stellar atmosphere and wind code FASTWIND. The low dispersion of O and Si abundances in B-type stars in the Orion OB1 association found in Paper I is confirmed. This is the first systematic comparison of results derived from the codes FASTWIND and ATLAS+DETAIL+SURFACE – commonly used in the analysis of massive stars – from a high quality set of stellar spectra. Moreover, this work constitutes the first step for further comparisons of elements to be incorporated in FASTWIND, that is also able to analyse more massive stars with winds.

The present work finds a significantly smaller abundance scatter (mainly in C, N, O, and Si, but also Fe) in Ori OB1 early B-type stars than previous works and similar scatter than CHL06 for Ne. The derived metal abundances are in excellent agreement with results of early B-type stars in the solar neighbourhood that define the Present-Day Cosmic Abundance Standard (PNB08). They also agree with data from an extended sample of stars in the solar vicinity (Nieva & Przybilla, in prep.). Despite the different state of these massive young stars and of older stars like the Sun in terms of Galactic chemical evolution, good agreement with the solar values is found – which poses the question of the origin of the Sun. Late-type stars in the region also present similar iron abundances.

This study, together with Paper I, has allowed us to establish a precise, homogeneous and reliable set of abundances for C, N, O, Ne, Mg, Si and Fe in the early B-type stars of Orion OB1. In a first application, the present results have facilitated constraints on the dust-phase composition of the Orion H II region derived in Paper II.

Acknowledgements. We would like to thank N. Przybilla for providing us with his updated versions of model atoms, valuable comments and careful reading of the manuscript. We also acknowledge M. Asplund, G. Stasińska, J. Puls and F. Najarro for their suggestions to improve the manuscript.

References

Asplund, M, Grevesse, N., Sauval, A. J. & Scott, P. 2009, ARA&A, 47, 481 (AGSS09)
Becker, S. R. 1998, in ASP Conf. Ser. 131, Boulder-Munich II: Properties of Hot, Luminous Stars, ed. I. Howarth, 137
Becker, S. R. & Butler, K. 1988a, A&A, 201, 232
Becker, S. R. & Butler, K. 1988b, A&AS, 76, 331
Becker, S. R. & Butler, K. 1989, A&A, 209, 244
Becker, S. R. & Butler, K. 1990a, A&A, 235, 326
Becker, S. R. & Butler, K. 1990b, A&AS, 84, 95
Biazzo, K., Randich, S., & Palla, F. 2010, arXiv:1010.1658
Blaauw, A. 1964, ARA&A, 2, 213
Brown, A. G. A., de Geus, E. J. & de Zeeuw, P. T. 1994, A&A, 289, 101
Butler, K. & Giddings, J. R. 1985, in Newsletter of Analysis of Astronomical Spectra, No. 9 (Univ. London)
Carigi, L., & Peimbert, M. 2010, Rev. Mexicana Astron. Astrofis., in press (arXiv:1004.0756)
Cowie, L. L., Songaila, A. & York, D. G. 1979, ApJ, 230, 469
Cunha, K., Hubeny, I. & Lanz, T. 2006, ApJ, 647, 143 (CHL06)
Cunha, K. & Lambert, D. L. 1992, ApJ, 399, 586 (CL92)
Cunha, K. & Lambert, D. L. 1994, ApJ, 426, 170 (CL94)
D'Orazi, V., Randich, S., Flaccomio, E. et al. 2009, A&A, 501, 973
Eber, F. & Butler, K. 1988, A&A, 202, 153
Gold, M. 1984, Diploma Thesis (University of Munich)
Hirsch, H. 2009, Ph.D. Thesis (University Erlangen-Nuremberg)
Hubeny, I. 1988, Comput. Phys. Commun., 52, 103
Hubeny, I. & Lanz. T. 1995, ApJ, 439, 875
Giddings, J. R. 1981, Ph.D. Thesis (University of London)
Gies, D. R. & Lambert, D. L. 1992, ApJ, 387, 673
González Hernández, J. I., Caballero, J. A., Rebolo, R. et al. 2008, A&A, 490, 1135
Grevesse, N. & Sauval, A. J. 1998, Space Sci. Rev., 85, 161
Gummersbach, C. A., Kaufer, A., Schaefer, et al. 1998, A&A, 338, 881
Kilian, J., Montenbruck, O., & Nissen, P. E. 1991, A&AS, 88, 101
Kilian, J. 1992, A&A, 262, 17
Kurucz, R. L. 1979, ApJS, 40, 1
Kurucz, R. L. 1993a, CD-ROM No. 2–12 (Cambridge, Mass.: SAO)
Kurucz, R. L. 1993b, CD-ROM No. 13 (Cambridge, Mass.: SAO)
Meléndez, J., Asplund, M., Gustafsson, B. & Yong, D. 2009, ApJ, 704, 66
Morel, T., Butler, K., Aerts, C., et al. 2007, A&A, 457, 651
Morel, T. & Butler, K. 2008, A&A, 487, 307
Nieva, M. F. & Przybilla, N. 2006, ApJ, 639, L39
Nieva, M. F. & Przybilla, N. 2007, A&A, 467, 295
Nieva, M. F. & Przybilla, N. 2008, A&A, 481, 199
Nieva, M.-F., & Przybilla, N. 2010a, Astronomical Society of the Pacific Conference Series, 425, 146
Nieva, M.-F., & Przybilla, N. 2010b, EAS Publications Series, 43, 167
Portegies Zwart, S. F. 2009, ApJ, 696, 13
Przybilla, N. 2005, A&A, 443, 293
Przybilla, N. & Butler, K. 2001, A&A, 379, 955
Przybilla, N. & Butler, K. 2004, ApJ, 609, 1181
Przybilla, N., Butler, K., Becker, S. R., et al. 2000, A&A, 359, 1085
Przybilla, N., Butler, K., & Kudritzki, R. P. 2001, A&A, 379, 936
Przybilla, N., Nieva, M. F., & Butler, K. 2008, ApJ, 688, L103
Puls, J., Urbaneja, M. A., Venero, R., et al. 2005, A&A, 435, 669
Reynolds, R. J. & Ogden, P. M. 1979, ApJ, 229, 942
Ramírez, I., Meléndez, J. & Asplund, M. 2009, A&A, 508, 17
Rybicki, G.B. & Hummer, D.G. 1991, A&A, 245, 171
Schaller, G., Schaerer, D., Meynet, G., & Maeder, A. 1992, A&AS, 96, 269
Schönrich & R., Binney, J. 2009, MNRAS, 396, 203
Simón-Díaz, S., Herrero, A., Esteban, C. & Najarro, F. 2006, A&A, 448, 351
Simón-Díaz, S. 2010, A&A, 510, A22 (Paper I)
Simón-Díaz S., Stasińska G., 2011, A&A, 526, A48 (Paper II)

Appendix A: An example of a global fit: HD 35299

To illustrate the global quality achieved in the spectral synthesis when a final self-consistent solution is considered, we show in Figs. A.3-A.7 the observed spectrum of an example star, HD 35299 and a synthetic spectrum computed using the stellar parameters and abundances indicated in Table 3. The spectral analysis was based on all Balmer and He lines and the metal lines marked at the bottom of the panels. For completeness purposes, all available lines from our present model atoms – even the lines excluded from the analysis for different reasons mentioned in Sect. 4 – and also from other atoms not analysed here in NLTE are included.

Surface gravities have been determined from the wings of the Balmer lines and via multiple metal ionization equilibria, that can be even more sensitive to this parameter. The cores of the hydrogen lines – which are not always well fitted – do not affect the analysis performed in this work, or at least, the effect is negligible.

The line identification is based on the lines included in our input for SURFACE. Evidently, some remaining lines/elements still need to be included to achieve complete coverage by the global spectrum synthesis. Identifications of the missing lines in the most important blue spectral region may be achieved on the basis of the spectral atlases of Kilian et al. (1991).

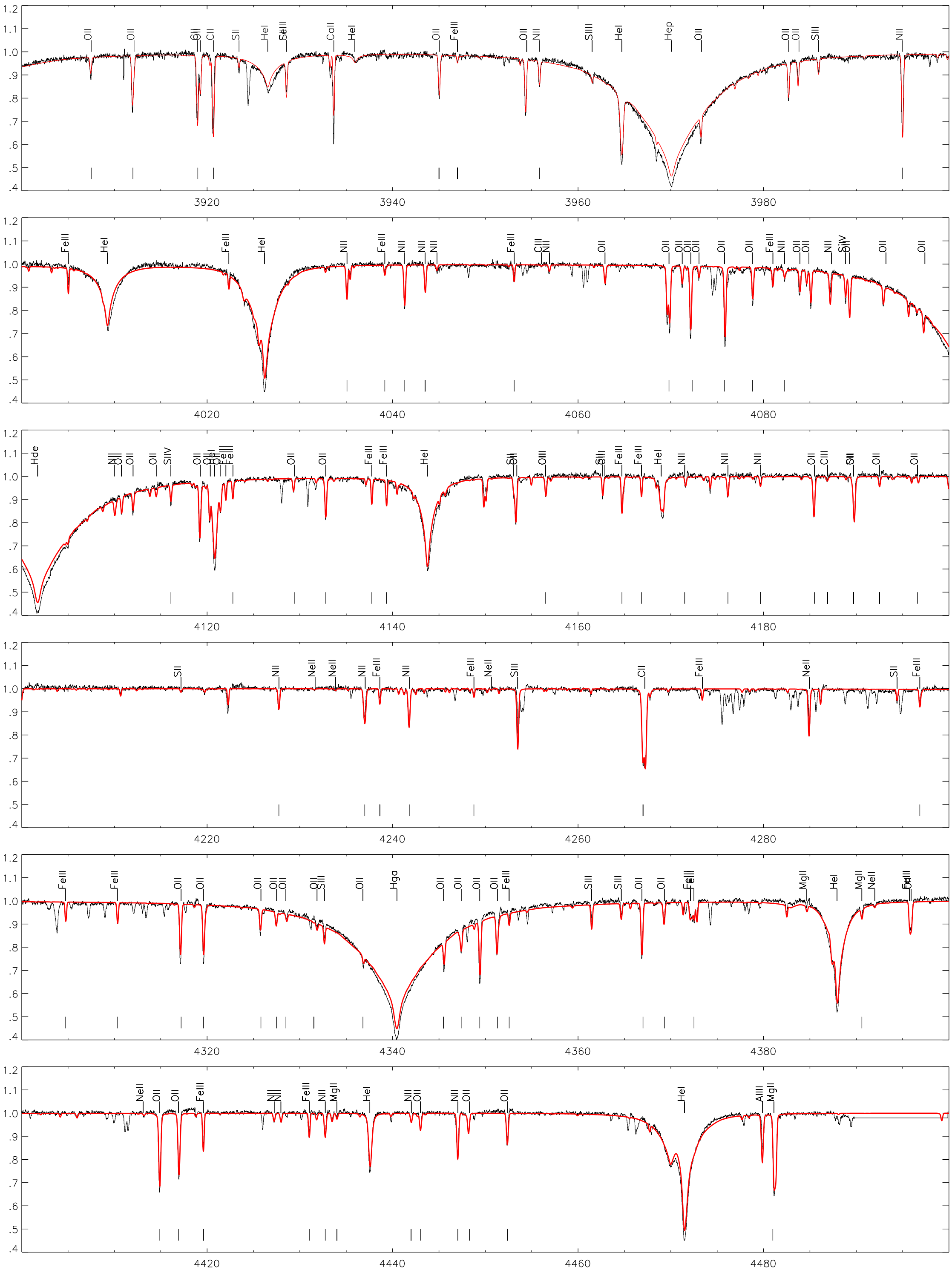

Fig. A.3. Comparison between the observed (black) and the model spectrum (red line) for the star HD 35299, for parameters and elemental abundances as given in Table 3. The spectral analysis was based on all Balmer and He lines and the metal lines marked at the bottom of the panels. Additional lines have been included in the global spectrum for visualization purposes, but the linelist is not complete. See the text for details.

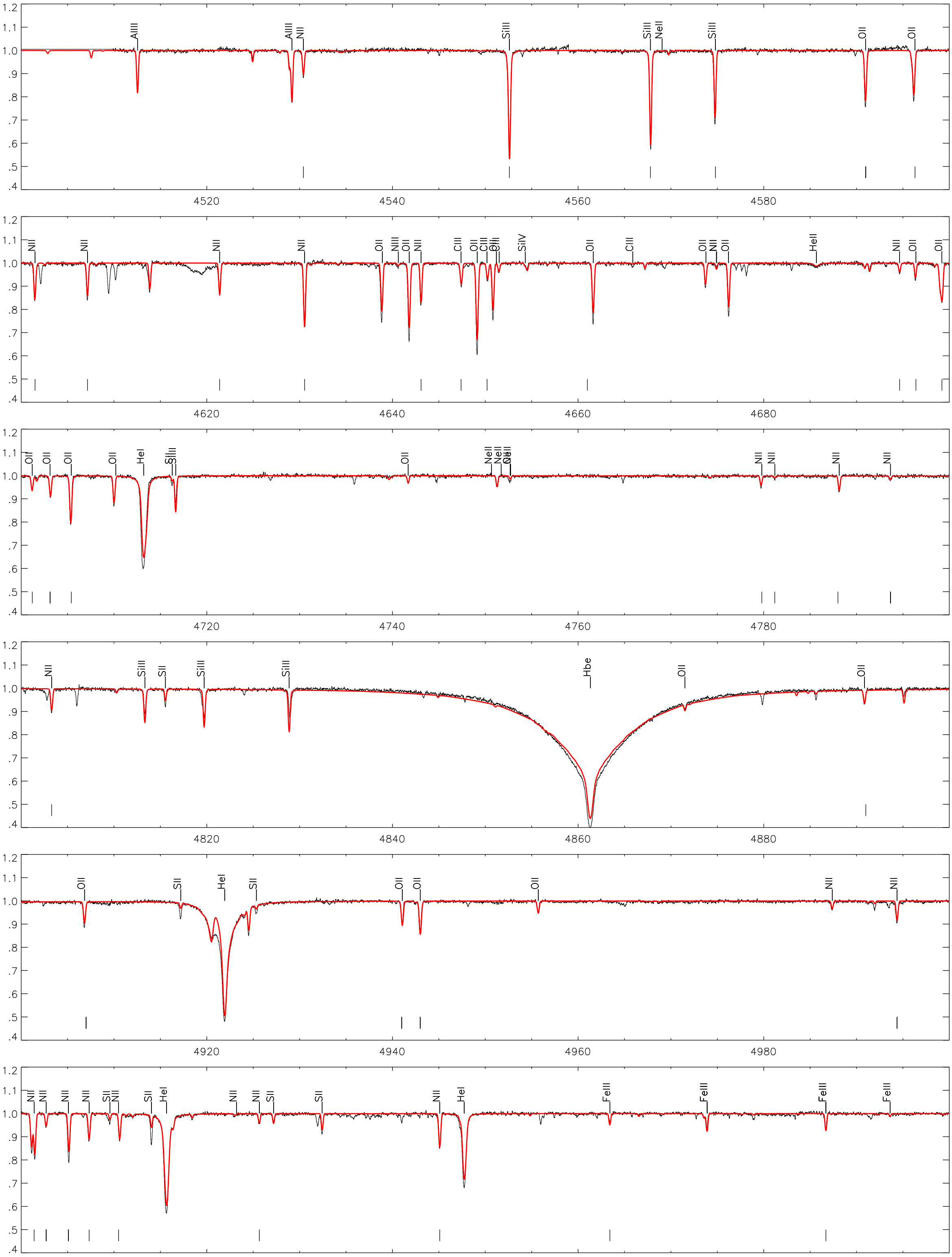

Fig. A.4. Same as Fig. A.3

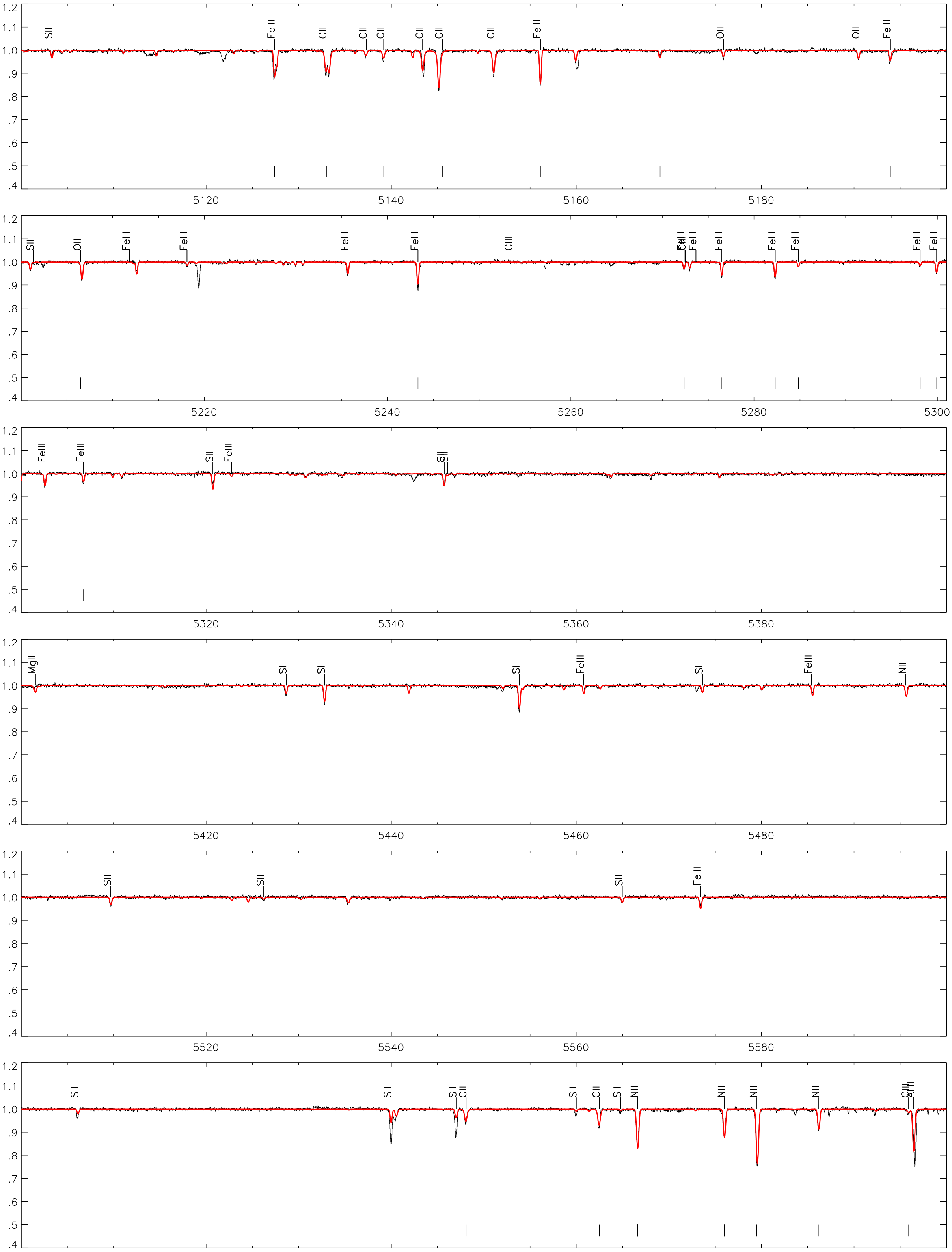

Fig. A.5. Same as Fig. A.3.

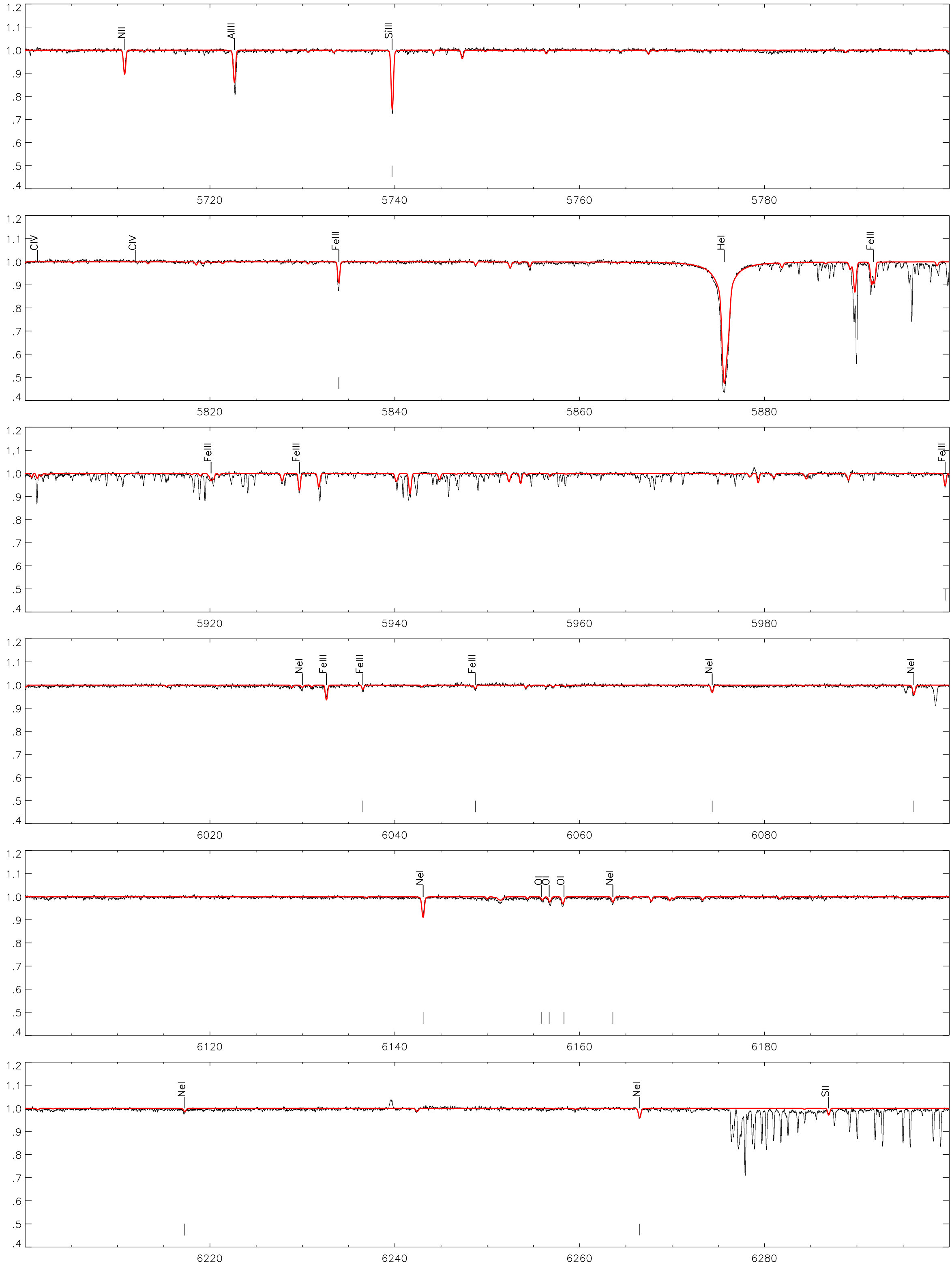

Fig. A.6. Same as Fig. A.3.

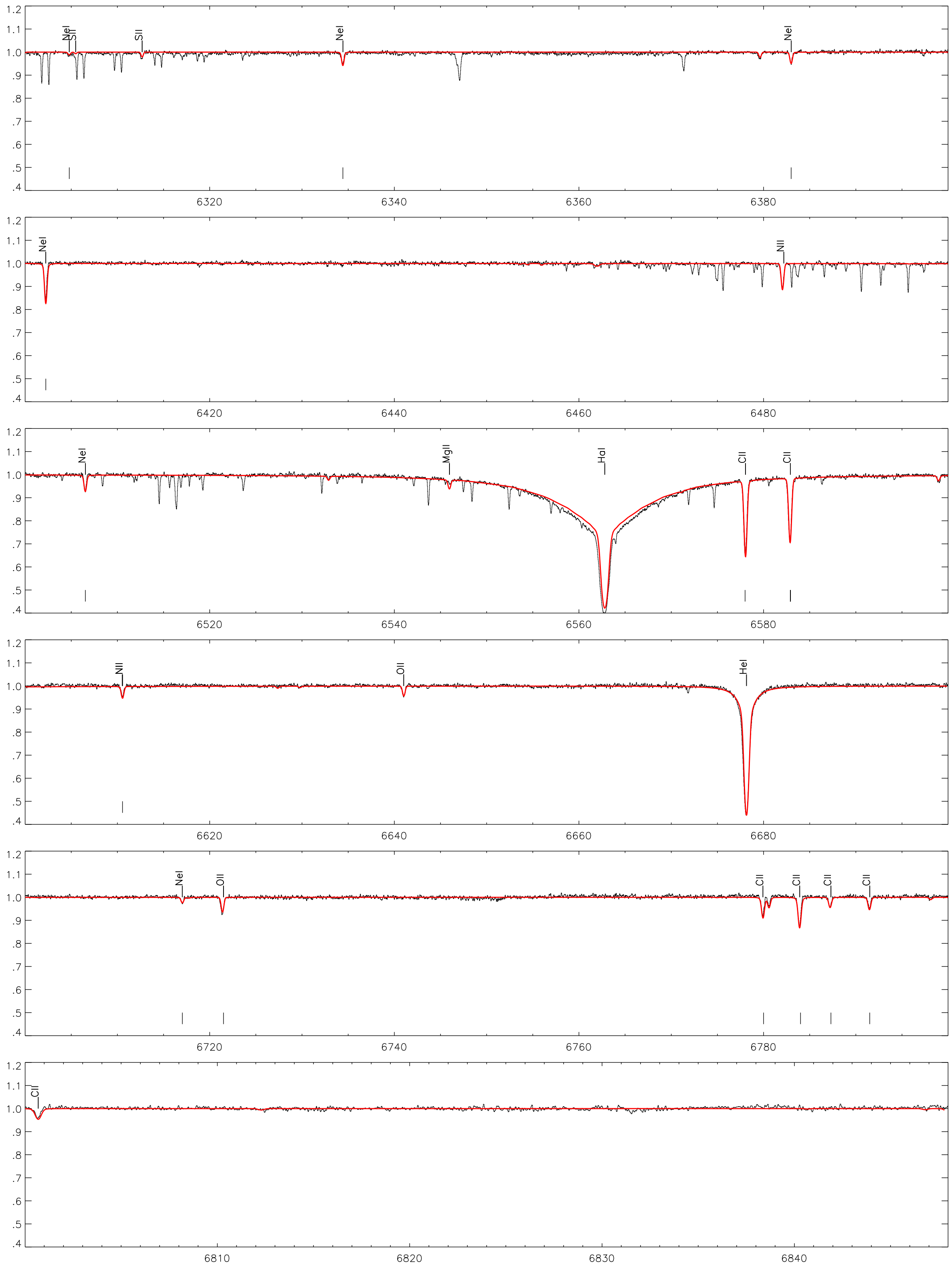

Fig. A.7. Same as Fig. A.3.